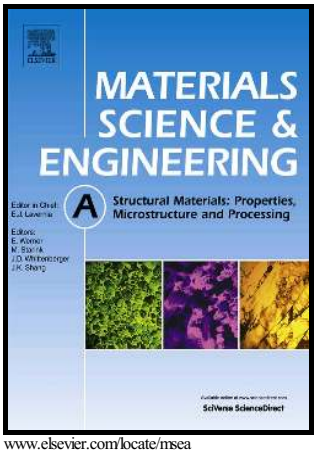

www.elsevier.com/locate/msea

High-strength aluminum-based composites reinforced with BN, AlB_2 and AlN particles fabricated via reactive spark plasma sintering of Al-BN powder mixtures

K.L. Firestein, S. Corthay, A.E. Steinman, A.T. Matveev, A.M. Kovalskii, I.V. Sukhorukova, D. Golberg, D.V. Shtansky

PII: S0921-5093(16)31365-X
DOI: http://dx.doi.org/10.1016/j.msea.2016.11.011
Reference: MSA34336

To appear in: *Materials Science & Engineering A*

Received date: 13 September 2016
Revised date: 3 November 2016
Accepted date: 4 November 2016

Cite this article as: K.L. Firestein, S. Corthay, A.E. Steinman, A.T. Matveev, A.M. Kovalskii, I.V. Sukhorukova, D. Golberg and D.V. Shtansky, High-strength aluminum-based composites reinforced with BN, AlB_2 and AlN particle fabricated via reactive spark plasma sintering of Al-BN powder mixtures *Materials Science & Engineering A* http://dx.doi.org/10.1016/j.msea.2016.11.011

High-strength aluminum-based composites reinforced with BN, AlB_2 and AlN particles fabricated via reactive spark plasma sintering of Al-BN powder mixtures

K.L. Firestein[a*], S. Corthay[a], A.E. Steinman[a], A.T. Matveev[a], A.M. Kovalskii[a], I.V. Sukhorukova[a], D. Golberg[b*], D.V. Shtansky[a*]

[a]*National University of Science and Technology "MISIS", Leninsky prospect 4, Moscow, 119049, Russian Federation*

[b]*World Premier International Center for Materials Nanoarchitectonics (WPI-MANA), National Institute for Materials Science (NIMS), Tsukuba, Namiki 1, Ibaraki 3050044, Japan*

const@firestein.ru

shtansky@shs.misis.ru

golberg.dmitri@nims.go.jp

[*]Corresponding authors. Tel.: +7 495 638 44 47 (K. Firestein);

[*]Corresponding author.

[*]Corresponding author. +7 499 236 66 29 (D. Shtansky)

Abstract

Light (density < 2.7 g×cm^{-3}) yet strong (tensile strength > 350 MPa) metal matrix composites (MMCs) are highly anticipated for aerospace and automotive industries. The MMCs application fields can be significantly expanded if they possess enhanced strength at elevated temperatures also. In the present study, Al-based composites loaded with either micro- or BN nanoparticles (BNMPs and BNNPs) with up to 10 wt.% of BN phase were produced *via* spark plasma sintering (SPS) of ball-milled Al-BN powder mixtures. A dramatic increase in the composite tensile strength compared to pure Al samples (up to 415 %) was demonstrated during tensile tests both at 20 °C and 500 °C. BNMPs were found to be a more preferred additive compared with BNNPs due to the formation of more homogeneous and uniform morphologies within the ball-milled powder mixtures and resultant SPS products. The most impressive tensile strength of 170 MPa at 500°C was achieved for an Al-7 wt.% BNMPs SPS composite, as compared to a value of only 33 MPa for a pure Al SPS-produced sample. The reinforcement mechanism was uncovered based on detailed X-ray diffraction analysis, differential scanning calorimetry, Raman spectroscopy, scanning and high-resolution transmission electron microscopy and energy-dispersion X-ray analysis. Microscale BN, AlB_2 and AlN inclusions acting within Al-matrices in the frame of Orowan strengthening mechanism, and pre-formed during ball-milling-induced pre-activation of Al-BN powder mixtures, finally crystallized during SPS processing and ensured the dramatically improved tensile strength and hardness of the resultant composites.

Keywords:
Mechanical characterization; Electron microscopy; Composites; Aluminium alloys; Powder metallurgy; Hardening;

1. Introduction

Aluminum is a lightweight, cheap and corrosion-resistant metal. It is widely used as a matrix for metal matrix composites (MMC) with a high specific strength [1]. Al-based MMCs (Al-MMCs) are promising materials for aerospace and automotive industries. Utilization of Al-MMCs can reduce the weight of construction, and allows for a significant reduction of fuel consumption [2,3]. Moreover, profound resistance to high temperature oxidation makes the usage of Al-MMCs possible at elevated temperatures (up to 500 °C) and even in oxidizing atmosphere [4].

Addition of various reinforcing agents can significantly improve mechanical properties of Al-based MMCs. There has been plenty of reports covering different aspects of fabrication and characterization of Al-based MMC filled with carbon nanotube (CNT), SiC, Al_2O_3, and TiB_2 inclusions [5–11].

Special attention should be paid to hexagonal BN (*h*-BN) nano- and microstructures as reinforcing agents in Al-based composites. Utilization of BN nanostructures with superb mechanical properties (tensile strength of BN nanotubes (BNNTs) and BN graphene-like sheets (BNGSs) were reported to be ~33 GPa and ~130 GPa, respectively [12,13]) provides a unique opportunity to produce a new type of Al-MMCs with significantly increased specific strength. For instance, a 3-fold increase in tensile strength was observed for the melt-spun ribbons with 5 wt.% BNNTs compared with pristine Al samples [14]. Compression strength of spark plasma sintered Al/BN samples was measured to be 216 MPa; that is 50 % higher than that of pure Al produced by the same technique [15]. Al-5 wt.% BNNTs MMCs produced through severe plastic deformation, i.e., high pressure torsion technique, showed a tensile strength value as high as 420 MPa [16]. Not only nanostructured *h*-BN was successfully used as a reinforcement phase for Al-MMCs, but, also *h*-BN microparticles (BNMPs) additions were able to provide a significant improvement in mechanical properties [17–20].

To the best of our knowledge, so far a very little experimental work has been carried out in regard to tensile strength of Al/BN composites, in particular during high-temperature deformations. In most cases, Al/BN composites were only characterized by standard compression [18], bending [20], and micropillar compression tests [15].

Thus the main aim of the present study was to conduct tensile tests on Al/BN composites for a wide range of nano- and micro-BN particle contents, from 0.5 to 10.0 wt.%, at room and elevated temperatures (500 ºC). Furthermore, we compared mechanical properties of Al/BN composites depending on the type and morphology of BN additives.

In our previous work [21] it was shown that mechanical properties of Al can be significantly improved through incorporating BN nanoparticles (BNNPs). Prior to fabrication of Al/BNNPs composites using spark plasma sintering (SPS), the Al and BNNPs powders were ultrasonically mixed. However, the main drawback of this technique was the structural heterogeneity of the sintered samples.

Therefore, in order to overcome this shortcoming, in the present work the Al/BN composites were first produced by high-energy ball milling (BM) followed by SPS processing. It was expected that the employment of high-energy BM would increase the homogeneity of a product and result in the further improvement of Al-MMC mechanical properties.

It is well known that BM can promote the reaction between Al and BN using the following scheme [22,23]:

$$3Al + 2BN = AlB_2 + 2AlN \quad (1)$$

The hard phases formed during this reaction (1), such as AlB_2 and AlN, pre-formed during preliminary BM and/or further SPS, can also contribute to the improved strength of Al-MMCs [24–27].

2. Materials and methods

2.1 Raw materials

Spherical Al powders with a purity of 99 wt. % and an average particle size of 10 μm were used to form the metallic matrices during BM and SPS. As reinforcing additives, commercial chemically pure BNNPs (“Plazmotherm”, Russian Federation) and BNMPs (“Reachem”, Russian Federation) were utilized. Micro- and nanoparticles had a thin flake shape with an average particle size of 4 μm and 20 nm, respectively.

2.2 Composite fabrication

The powder mixtures were prepared using a high energy ball mill mixer E_{max} (“Retsch GmbH”, Germany). Mixing was conducted in ZrO_2 jars filled with ZrO_2 balls. During mixing, a

ball/powder weight ratio was 10:1 and a rotation speed was maintained at 800 rpm. To prevent Al oxidation, mixing was carried out in an Ar atmosphere. The powder mixtures were then sintered by SPS using a "LABOX 650" ("Sinter Land Inc.", Japan) press. Vacuum sintering was carried out in a graphite die with an inner diameter of 30 mm under the following technological parameters: sintering temperature – 600 ^{o}C, heating rate – 60 ^{o}/min, isothermal holding at the sintering temperature – 60 min and sintering pressure – 50 MPa. Once the samples reached the temperature of 320 ^{o}C, heating was stopped to maintain the temperature for 5 min. This was done in order to remove all volatiles, such as water and absorbed gases. When heating had been completed, sintering pressure was applied to the samples. The scheme of SPS process also showing the temperature-time and pressure-time plots is presented in Figs. S1a and S1b (see Supporting Information). As a result, tablet-shape 6 mm thick samples, 30 mm in diameter, were produced.

In total, 12 Al-MMC samples with 0.5, 1.5, 3.0, 4.5, 7 and 10 wt.% of h-BN nano- and microparticles were sintered. Hereafter they are abbreviated as Al-0.5BNMP, Al-1.5BNMP, Al-3.0BNMP, Al-4.5BNMP, Al-7.0BNMP, Al-10.0BNMP and Al-0.5BNNP, Al-1.5BNNP, Al-3.0BNNP, Al-4.5BNNP, Al-7.0BNNP, Al-10.0BNNP. Pure Al samples fabricated under the same BM and SPS conditions were used as references.

The theoretical density of Al MMC with 0.5, 1.5, 3.0, 4.5, 7, and 10 wt.% of h-BN was 2.687, 2.682, 2.675, 2.667, 2.654, 2.639 g×cm^{-3} respectively. The density of all produced composites was controlled using a hydrostatic weighing technique. The actual density was > 97% of the theoretical density.

2.3 Mechanical testing

Tensile tests were performed for all samples both at room temperature (RT) and at 500 ºC. Each sintered sample was initially cut into several stripes using a "Secotom 50" ("Struers Inc", Denmark) precision cutting machine and then each strip was tooled to a dumb-bell shape (Fig. S2, Supporting Information) using a "Chmer GX-320L" ("Chmer", Taiwan) electric discharge cutting machine. For each sample, at least 4 test pieces were tested and an average strength was calculated. Tensile tests were carried out using a universal testing machine "Shimadzu AG-X Series" ("Shimadzu Corp.", Japan) with a maximal load of 20 kN. All the samples were loaded at a strain rate of $0.83 \cdot 10^{-4}$ m/s until complete failure. To examine the high temperature tensile strength, the analogous mechanical tests were carried out in a resistive furnace pre-heated to 500 ^{o}C.

Microhardness of the synthesized composites was measured *via* Vickers hardness tests using a DuraScan 70 microhardness tester ("Emco-Test Prüfmaschinen GmbH", Austria).

2.4 Characterization

The microstructures and chemical compositions of the initial powder mixtures and sintered samples were studied by scanning electron microscopy (SEM) using a "JEOL F7600" ("Jeol Ltd.", Japan) device equipped with backscattered electrons (BSE) and energy dispersive X-ray spectroscopy (EDS) detectors and by transmission electron microscopy (TEM) using "JEOL 2100" instrument ("Jeol Ltd.", Japan) equipped with EDS spectrometer. The Al/BN samples for microstructure analysis were polished using a "Tegramin" preparation system ("Struers Inc.", Denmark). XRD analysis was carried out using a "DRON-3" diffractometer (Russia). Phase compositions of powder mixtures were evaluated using confocal Raman spectroscopy using a "NTEGRA Spectra" instrument (NT-MDT, Russia). Reaction between Al and *h*-BN powders in an Ar atmosphere was studied *via* differential scanning calorimetry (DSC) technique using a "STA 449 F1 Jupiter" DSC (NETZSCH-Gerätebau GmbH, Germany).

3. Results and discussion

3.1 Mechanical properties

The relationships between the room temperature mechanical properties of the composites (ultimate tensile strength – UTS, and yield strength – $\sigma_{0.2)}$ and BN phase contents are shown in Figs. 1a and 1b. The tensile strength of both composite types showed an analogous behavior versus an amount of BN additive. It reached a maximum value of 386 MPa at 4.5 and 7 wt.% of BN for Al-BNMPs and Al-BNNPs, respectively. Thus, the samples reinforced with nano/micro BN additives demonstrated 320 % tensile strength increase compared with the 94 MPa value for pristine Al sintered without the BM activation stage and 130 % increase compared with the 167 MPa value for pristine Al sintered with BM stage. When the concentration of BN phases had been further increased to 10 wt.%, the tensile strength decreased to 235 and 257 MPa for Al-10BNMP and Al-10BNNP composites, respectively.

Due to a small size of the dumb-bell test pieces, the exact definition of the Young's modulus and relative elongation during the tensile tests were difficult. Therefore in the present

study, the ductility of the composites was qualitatively evaluated from the shapes of the stress-displacement curves presented in Fig. 1c (for selective samples with the best mechanical performances) and in Figs. S3 and S4 (Supporting Information) for all samples. For both types of BN additives, the ductility decreased with increasing BN concentration. Ball milling leads to significant improvement in tensile strength and decrease in ductility of SPS sintered samples. Note that a small addition of BN leads to simultaneous improvement of UTS and ductility of pure Al after BM stage.

Fig. 2 compares the tensile strength values of Al-BNMPs and Al-BNNPs samples with different BN contents tested at 500 °C. The maximum strength was observed for a sample with 7 wt.% of BNMPs. This is 415 % higher than the tensile strength of pure Al, and 190 % higher compared with that of pure Al produced using the BM stage. It is worth noting that the tensile strength of the Al-7.0BNMPs composite at 500 ^{o}C was even higher than the strength of pure Al at room temperature. The stress-displacement curves for all samples obtained during high temperature tensile tests are presented in Figs. S5 and S6 (Supporting information).

The results of Vickers hardness tests on all composites are shown in Fig. 3. For both types of reinforcements, the hardness increased with increasing BN content. The maximum hardness of ~135 HV was observed for Al-10BNMP and Al-10BNNP samples. The obtained results showed that the hardness had increased by 380 % and 210 % with respect to pure Al samples fabricated with and without BM stages, respectively.

3.2 Structure and phase composition

Microstructure of raw materials used for SPS is presented in Fig. 4. The BNMPs with a flake-like shape had a size of about 5 μm and a thickness of 200-300 nm (Fig. 4a). The BNNPs are significantly agglomerated forming two-dimensional "nanopetals" with a size of 20-30 nm (Fig. 4b).

Figures 5a and 5b depict the selected SEM micrographs with the corresponding results of EDS analysis of the Al-BN powder mixtures with 7 wt. % of BNMPs and BNNPs. After BM stage, large composite agglomerates with a size of > 100 μm were formed. The EDS analysis (Figs. 5a and 5b (insets 1 and 2)) confirmed the presence of B and N within the agglomerates. The phase composition of powder mixtures after BM stage was detailed using XRD analysis. The mixtures were preliminary etched in a 10 % water solution of HCl for 3 h to dissolve Al. The XRD pattern of the powder mixture after etching (Fig. S7, Supporting Information) demonstrated only peaks from the BN and $AlCl_3x6H_2O$ phases (a water-soluble product of the

reaction between Al and HCl). In addition, the powder mixtures were studied by Raman spectroscopy. This revealed a characteristic band at 930 cm^{-1} corresponding to the AlB_2 phase (Fig. 5, inset 3) and thus confirmed its formation during BM. The E_{2g} band of hexagonal BN at 1365 cm^{-1} is also clearly visible. There are no peaks corresponding to AlB_2 on XRD patterns because only minor traces of AlB_2 were pre-formed during the BM stage.

In order to investigate the microstructures of powder mixtures after BM, the samples with 7 wt.% of BNMPs and BNNPs were mounted in resin and then the cross-sectional pieces were prepared using polishing. The SEM micrographs of Al-BN agglomerates after BM are presented in Figs. 5c and 5d. BN phase was found to be uniformly distributed within the Al matrices. In case of BNMPs, the stucture looks more uniform and homogeneous.

The microctructures and elemental composition of SPS-processed Al-4.5BNMP and Al-4.5BNNP composites were also studied by SEM and EDS (Fig. 6). Both Al-4.5BNMP and Al-4.5BNNP samples showed a relativly large (0.5 - 2 μm) dark inclusions (marked by arrows in Fig. 6). Their chemical composition was close to that of an AlB_2 phase (in agreement with the Raman data). Note that the smaller inclusions with a size of 100 nm were also observed, but their chemical analysis using EDS is difficult because of spatial resolution limitations. The white dots seen on the images correspond to SiO_2–traces from the polishing suspension, which was used during the sample preparation procedure. Importantly, the significant difference between the Al-4.5BNMP and Al-4.5BNNP samples was apparent. The former structure was more uniform with a size of AlB_2 inclusions of less than 0.5 μm, while the size of AlB_2 particles in the latter composite was up to 2 μm. The observed difference can be well explained by the structure of the initial powder mixtures after BM, i.e., the less homogeneous composite agglomerates after BM result in less homogeneous final SPS products.

Unlike AlB_2, AlN phase did not form large inclusions and therefore was not visible in SEM micrographs. Note, however, that during a reaction between Al and BN, both phases, i.e., AlB_2 and AlN, should be formed. In order to study the phase composition of SPS samples in more detail, their final XRD analysis was performed. The XRD patterns of the Al-4.5BNMP composite is presented in Fig. 7. Apart from the peaks originated from h-BN and AlB_2 phases, additionally observed XRD peaks at 2θ of 33.2°, 38.8°, 59.7° indeed correspond to (100), (101) and (110) planes of the AlN phase.

In order to better understand the composite microstructure, a sample with the best mechanical properties (Al-4.5BNMP) was thoroughly studied by TEM (Fig. 8). High-angle annular dark-field (HAADF) image (Fig. 8a) of the Al-4.5BNMP composite shows that the material consists of big grains with a size of 300-600 nm and small black elongated inclusions with a size < 100 nm. EDS analysis reveals that two type of inclusions, namely AlB_2 that form

big grains with a size close to that of Al grains (see point 2 in Fig. 8), and mixed BN and AlN small black inclusions (see point 3 in Fig. 8) exist within the Al matrix (grain size of Al – 300-600 nm, see point 1 in Fig. 8). High-resolution TEM (HRTEM) image of an individul black inclusion is depicted in Fig. 8d. It consists of turbostratic BN with the additions of AlN; the particle size is ~10-20 nm. HRTEM image of AlN particle is illustrated in Fig. 8e. The distance between fringes is 0.264 nm; this agrees well with the (100) lattice spacing in AlN.

3.3 DSC analysis of powder mixtures

XRD analysis (Fig. 7) confirmed that the reaction (1) had indeed proceeded during SPS processing. To study this reaction in more details, DSC analysis of the Al-7.0BNMP powder mixture after BM was performed. A DSC curve is shown in Fig. 9. The exothermic peak corresponding to the above-mentioned reaction between Al and BN is clearly visible. The reaction takes place in a temperature range between 480 °C and 575 °C. The heating rate during DSC analysis was 10 °C/min, that is 6 times slower than that during SPS process. Note that a long isothermal hold (60 min) at 600 °C appears to be sufficient to reach the equilibrium during SPS. The presence of h-BN in composites after SPS can be attributed to the *h*-BN leftover which was not fully "activated" during BM.

3.4 Discussion

The mechanical tests demonstrated that the BM-activated SPS Al-BN composites possess high hardness and tensile strength at room temperature and at 500 °C (Figs. 1-3). Interestingly enough, downsizing the BN particles, i.e., the utilization of BNNPs instead of BNMPs did not lead to an improvement of mechanical properties of Al-BN MMCs. Moreover, using BNMPs allow us to reach the maximum tensile strength at the smaller BN phase contents. This can be explained due to poorer homogeneity in the powder mixtures after BM stage (Fig. 5c and 5d) and within sintered composites (Fig. 6) for Al-BNNPs composites compared with their Al-BNMPs counterparts. The latter fact can be understood due to a difference between lubrication properties of h-BN with different morphologies. It is known that h-BN microparticles can act as a solid lubricant [28–30], but notable agglomeration of BNNPs (Fig. 4b) and sufficient quantities of absorbed gases on their highly developed surfaces may result in an adverse effect of h-BN lubrication characteristics compared with BNMPs.

High energy BM promoted the reaction (1) between Al and h-BN to form AlB_2 and AlN phases. In fact, the traces of AlB_2 phase observed in the powder mixtures support this conclusion (Fig. 5, inset 3). Note though, that in the early work [31] the traces of AlB_2 and AlN phases were only found in Al-BN composites produced without BM after isothermal holding at 600 °C for 300 min. The size of these inclusions was less than 20 nm. In contrast, the combination of BM and SPS leads to the formation of a significant amount of AlB_2 and AlN phases with a size of AlB_2 of > 200 nm (and up to 2 μm).

The DSC analysis (Fig. 9) also confirmed the on-going reaction (1) in a temperature range of 480-575 °C. The result of DSC agrees well with the previous studies [22,23] where the influence of BM on this reaction has been investigated. The main conclusion was that the reaction had not occurred without BM treatment. It is worth noting that the exothermic peak corresponding to the reaction between Al and BN became noticeable on the DSC curves only after 12 h of BM [22], whereas in the present study this peak was already observed after 2 h of BM.

Reinforcing Al-BNMPs and Al-BNNPs composites compared with pure Al could be attributed to the two strengthening mechanisms: (i) Orowan strengthening due to the presence of hard inclusions (BN, AlB_2, and AlN) in an Al matrix; and (ii) Hall-Petch strengthening due to reducing of Al grain size during BM. The Hall-Petch strengthening appears to be responsible for an increase in pure Al tensile strength after BM. To shed an additional light on the exact strengthening mechanism, we investigated the structure of Al matrix for an Al-0.5BNMP sample (Fig. S8, Supporting Information). The analysis indicated that the grain size of Al was about 500 nm; this is close to a grain size of Al-4.5BNMP (Fig 8a), therefore the Al matrix grain size did not noticeably change with increasing BN contents. This suggests that the Orowan mechanism is primarily responsible for the observed dramatic strengthening of Al-BNMPs and Al-BNNPs composites.

To date, many works have been dedicated to Al-based composites reinforced with ceramic nano- and/or microparticles. Nevertheless, a well-balanced comparison of the results is complicated due to a variety of methods used for mechanical property measurements. Thus, in the present work we only compare the values of the ultimate tensile strength reported till now in the literature for the samples fabricated using powder metallurgy routes. These results are shown in Table 1.

It is apparent that the reinforcing effect strongly depends on the processing technique utilized. Thus, it is important to exactly know the mechanical properties of a pure Al matrix without reinforcing additivities which has been synthesized in the same way. For instance, tensile strength of pure Al after high-pressure torsion was 221 MPa [16], while tensile strength

of pure Al after BM and SPS in the present work was 167 MPa. Therefore, the strength increase of a composite (in percentage) with respect to the pure Al fabricated using the analogous technique is shown in the right column of Table 1. The best composite material obtained in the present study demonstrated a 130 % improvement, which is among the best results presented in Table 1. It is also emphasized that relatively cheap BNMPs and a single stage densification technique employed in the present study are particularly economically efficient for future applications. Finally, it is noted that mechanical property improvement of conventional Al-based alloys, like 6061, 7075, 2014 etc., may also be expected under using the developed BM-SPS route, but unlikely at warm and high temperatures because of lowering of the alloy melting points compared to Al-MMCs.

4. Conclusions

Twelve Al-MMC samples with 0.5, 1.5, 3.0, 4.5, 7 and 10 wt.% of BNNPs and BNMPs were fabricated using SPS technique. Tensile tests carried out at room and elevated (500^{o}C) temperatures, as well as hardness measurements, showed similar trends of reinforcements for Al-BNNPs and Al-BNMPs composites with an increase in BN phase contents. The highest tensile strengths 386 MPa at room temperature and 170 MPa at 500 ^{o}C were recorded for the composites with 4.5 and 7.0 wt.% of BNMPs, respectively. Detailed structural investigation revealed that the samples with BNMPs had possessed more homogeneous structures than those with BNNPs, hereby ensuring their better mechanical performance. Summarizing DSC, Raman, XRD, SEM, EDS and HRTEM data obtained for powder mixtures and resultant composites, it was documented that employed powder mixture activation *via* ball milling had effectively promoted the reaction between Al and BN phases. During following SPS processing the uniformly distributed inclusions of AlB_2 (300-500 nm in size) and small particles (less than 100 nm in size) consisting of turbostratic BN mixed with an AlN phase finally crystallized. These ensured the significant strengthening of Al-BN-MMCs.

Acknowledgements

The work was supported by the Ministry of Education and Science of the Russian Federation (Increase Competitiveness Program of NUST «MISiS» No. K2-2015-067 and State task 11.1077.2014/K).

References

[1] R. Casati, M. Vedani, Metal Matrix Composites Reinforced by Nano-Particles—A Review, Metals (Basel). 4 (2014) 65–83. doi:10.3390/met4010065.

[2] S. V. Prasad, R. Asthana, Aluminum metal-matrix composites for automotive applications: Tribological considerations, Tribol. Lett. 17 (2004) 445–453. doi:10.1023/B:TRIL.0000044492.91991.f3.

[3] S. Rawal, Metal-matrix composites for space applications, Jom. 53 (2001) 14–17. doi:10.1007/s11837-001-0139-z.

[4] H.M. Zakaria, Microstructural and corrosion behavior of Al/SiC metal matrix composites, Ain Shams Eng. J. 5 (2014) 831–838. doi:10.1016/j.asej.2014.03.003.

[5] S.R. Bakshi, D. Lahiri, A. Agarwal, Carbon nanotube reinforced metal matrix composites - a review, Int. Mater. Rev. 55 (2010) 41–64. doi:10.1179/095066009X12572530170543.

[6] L. Zhang, H. Xu, Z. Wang, Q. Li, J. Wu, Mechanical properties and corrosion behavior of Al/SiC composites, J. Alloys Compd. 678 (2016) 23–30. doi:10.1016/j.jallcom.2016.03.180.

[7] E. Darmiani, I. Danaee, M.A. Golozar, M.R. Toroghinejad, A. Ashrafi, A. Ahmadi, Reciprocating wear resistance of Al-SiC nano-composite fabricated by accumulative roll bonding process, Mater. Des. 50 (2013) 497–502. doi:10.1016/j.matdes.2013.03.047.

[8] B.F. Schultz, J.B. Ferguson, P.K. Rohatgi, Microstructure and hardness of Al_2O_3 nanoparticle reinforced Al-Mg composites fabricated by reactive wetting and stir mixing, Mater. Sci. Eng. A. 530 (2011) 87–97. doi:10.1016/j.msea.2011.09.042.

[9] Y. Zhou, H. Wang, An $Al@Al_2O_3@SiO_2$/polyimide composite with multilayer coating structure fillers based on self-passivated aluminum cores, Appl. Phys. Lett. 102 (2013) 132901. doi:10.1063/1.4798837.

[10] Q. Gao, S. Wu, S. Lü, X. Duan, P. An, Preparation of in-situ 5 vol% TiB_2 particulate reinforced Al-4.5Cu alloy matrix composites assisted by improved mechanical stirring process, Mater. Des. 94 (2016) 79–86. doi:10.1016/j.matdes.2016.01.023.

[11] Y.C. Kang, S.L.I. Chan, Tensile properties of nanometric Al_2O_3 particulate-reinforced aluminum matrix composites, Mater. Chem. Phys. 85 (2004) 438–443. doi:10.1016/j.matchemphys.2004.02.002.

[12] X. Wei, M.S. Wang, Y. Bando, D. Golberg, Tensile tests on individual multi-walled boron nitride nanotubes, Adv. Mater. 22 (2010) 4895–4899. doi:10.1002/adma.201001829.

[13] C. Lee, X. Wei, J.W. Kysar, J. Hone, Measurement of the Elastic Properties and Intrinsic Strength of Monolayer Graphene, Science 321 (2008) 385–388. doi:10.1126/science.1157996.

[14] M. Yamaguchi, J. Bernhardt, K. Faerstein, D. Shtansky, Y. Bando, I.S. Golovin, H.R. Sinning, D. Golberg, Fabrication and characteristics of melt-spun Al ribbons reinforced with nano/micro-BN phases, Acta Mater. 61 (2013) 7604–7615. doi:10.1016/j.actamat.2013.08.062.

[15] D. Lahiri, A. Hadjikhani, C. Zhang, T. Xing, L.H. Li, Y. Chen, A. Agarwal, Boron nitride nanotubes reinforced aluminum composites prepared by spark plasma sintering: Microstructure, mechanical properties and deformation behavior, Mater. Sci. Eng. A. 574 (2013) 149–156. doi:10.1016/j.msea.2013.03.022.

[16] Y. Xue, B. Jiang, L. Bourgeois, P. Dai, M. Mitome, C. Zhang, M. Yamaguchi, A. Matveev, C. Tang, Y. Bando, K. Tsuchiya, D. Golberg, Aluminum matrix composites reinforced with multi-walled boron nitride nanotubes fabricated by a high-pressure torsion technique, Mater. Des. 88 (2015) 451–460. doi:10.1016/j.matdes.2015.08.162.

[17] Y. Du, S. Li, K. Zhang, K. Lu, BN/Al composite formation by high-energy ball milling, Scr. Mater. 36 (1997) 7–14. doi:10.1016/S1359-6462(96)00335-1.

[18] C. Chen, L. Guo, J. Luo, J. Hao, Z. Guo, A.A. Volinsky, Aluminum powder size and microstructure effects on properties of boron nitride reinforced aluminum matrix composites fabricated by semi-solid powder metallurgy, Mater. Sci. Eng. A. 646 (2015) 306–314. doi:10.1016/j.msea.2015.08.081.

[19] M. V. Gorshenkov, S.D. Kaloshkin, V. V. Tcherdyntsev, V.D. Danilov, V.N. Gulbin, Dry sliding friction of Al-based composites reinforced with various boron-containing particles, in: J. Alloys Compd., 2012: pp. S126–S129. doi:10.1016/j.jallcom.2011.12.065.

[20] G.A. Sweet, M. Brochu, R.L. Hexemer, I.W. Donaldson, D.P. Bishop, Consolidation of aluminum-based metal matrix composites via spark plasma sintering, Mater. Sci. Eng. A. 648 (2015) 123–133. doi:10.1016/j.msea.2015.09.027.

[21] K.L. Firestein, A.E. Steinman, I.S. Golovin, J. Cifre, E.A. Obraztsova, A.T. Matveev, A.M. Kovalskii, O.I. Lebedev, D. V. Shtansky, D. Golberg, Fabrication, characterization, and mechanical properties of spark plasma sintered Al-BN nanoparticle composites, Mater. Sci. Eng. A. 642 (2015) 104–112. doi:10.1016/j.msea.2015.06.059.

[22] Z.P. Xia, Z.Q. Li, C.J. Lu, B. Zhang, Y. Zhou, Structural evolution of Al/BN mixture during mechanical alloying, J. Alloys Compd. 399 (2005) 139–143. doi:10.1016/j.jallcom.2005.03.087.

[23] I. V. Povstugar, A.N. Streletskii, D.G. Permenov, I. V. Kolbanev, S.N. Mudretsova, Mechanochemical synthesis of activated Me-BN (Me{double bond, long}Al, Mg, Ti) nanocomposites, J. Alloys Compd. 483 (2009) 298–301. doi:10.1016/j.jallcom.2008.07.185.

[24] N. Mathan Kumar, S. Senthil Kumaran, L.A. Kumaraswamidhas, Wear behaviour of Al 261 8 alloy reinforced with Si_3N_4, AlN and ZrB_2 in situ composites at elevated temperatures, Alexandria Eng. J. 55 (2016) 19–36. doi:10.1016/j.aej.2016.01.017.

[25] L. Yuan, J. Han, J. Liu, Z. Jiang, Mechanical properties and tribological behavior of aluminum matrix composites reinforced with in-situ AlB_2 particles, Tribol. Int. 98 (2016) 41–47. doi:10.1016/j.triboint.2016.01.046.

[26] R. Kayikci, Fabrication and properties of functionally graded Al/AlB_2 composites, J. Compos. Mater. (2015). doi:10.1177/0021998314541490.

[27] K. Mizuuchi, K. Inoue, Y. Agari, T. Nagaoka, M. Sugioka, M. Tanaka, T. Takeuchi, J.I. Tani, M. Kawahara, Y. Makino, M. Ito, Processing and thermal properties of Al/AlN composites in continuous solid-liquid co-existent state by spark plasma sintering, Compos. Part B Eng. 43 (2012) 1557–1563. doi:10.1016/j.compositesb.2011.06.017.

[28] Z. Pawlak, T. Kaldonski, R. Pai, E. Bayraktar, A. Oloyede, A comparative study on the tribological behaviour of hexagonal boron nitride (*h*-BN) as lubricating micro-particles-An additive in porous sliding bearings for a car clutch, Wear. 267 (2009) 1198–1202. doi:10.1016/j.wear.2008.11.020.

[29] B. Chen, Q. Bi, J. Yang, Y. Xia, J. Hao, Tribological properties of solid lubricants (graphite, *h*-BN) for Cu-based P/M friction composites, Tribol. Int. 41 (2008) 1145–1152. doi:10.1016/j.triboint.2008.02.014.

[30] Y. Kimura, T. Wakabayashi, K. Okada, T. Wada, H. Nishikawa, Boron nitride as a lubricant additive, Wear. 232 (1999) 199–206. doi:10.1016/S0043-1648(99)00146-5.

[31] D. Lahiri, V. Singh, L.H. Li, T. Xing, S. Seal, Y. Chen, A. Agarwal, Insight into reactions and interface between boron nitride nanotube and aluminum, J. Mater. Res. (2012) 1–11. doi:10.1557/jmr.2012.294.

[32] Z.Y. Liu, K. Zhao, B.L. Xiao, W.G. Wang, Z.Y. Ma, Fabrication of CNT/Al composites with low damage to CNTs by a novel solution-assisted wet mixing combined with powder metallurgy processing, Mater. Des. 97 (2016) 424–430. doi:10.1016/j.matdes.2016.02.121.

[33] H. Choi, J. Shin, B. Min, J. Park, D. Bae, Reinforcing effects of carbon nanotubes in structural aluminum matrix nanocomposites, J. Mater. Res. 24 (2009) 2610–2616. doi:10.1557/jmr.2009.0318.

[34] X. Yang, T. Zou, C. Shi, E. Liu, C. He, N. Zhao, Effect of carbon nanotube (CNT) content on the properties of in-situ synthesis CNT reinforced Al composites, Mater. Sci. Eng. A. 660 (2016) 11–18. doi:10.1016/j.msea.2016.02.062.

[35] H. Kwon, M. Estili, K. Takagi, T. Miyazaki, A. Kawasaki, Combination of hot extrusion

and spark plasma sintering for producing carbon nanotube reinforced aluminum matrix composites, Carbon N. Y. 47 (2009) 570–577. doi:10.1016/j.carbon.2008.10.041.

[36] R. Casati, X. Wei, K. Xia, D. Dellasega, A. Tuissi, E. Villa, M. Vedani, Mechanical and functional properties of ultrafine grained Al wires reinforced by nano-Al_2O_3 particles, Mater. Des. 64 (2014) 102–109. doi:10.1016/j.matdes.2014.07.052.

[37] M. Zabihi, M.R. Toroghinejad, A. Shafyei, Application of powder metallurgy and hot rolling processes for manufacturing aluminum/alumina composite strips, Mater. Sci. Eng. A. 560 (2013) 567–574. doi:10.1016/j.msea.2012.09.103.

[38] M. Rahimian, N. Parvin, N. Ehsani, Investigation of particle size and amount of alumina on microstructure and mechanical properties of Al matrix composite made by powder metallurgy, Mater. Sci. Eng. A. 527 (2010) 1031–1038. doi:10.1016/j.msea.2009.09.034.

[39] M. Alizadeh, M.H. Paydar, Fabrication of nanostructure Al/SiCP composite by accumulative roll-bonding (ARB) process, J. Alloys Compd. 492 (2010) 231–235. doi:10.1016/j.jallcom.2009.12.026.

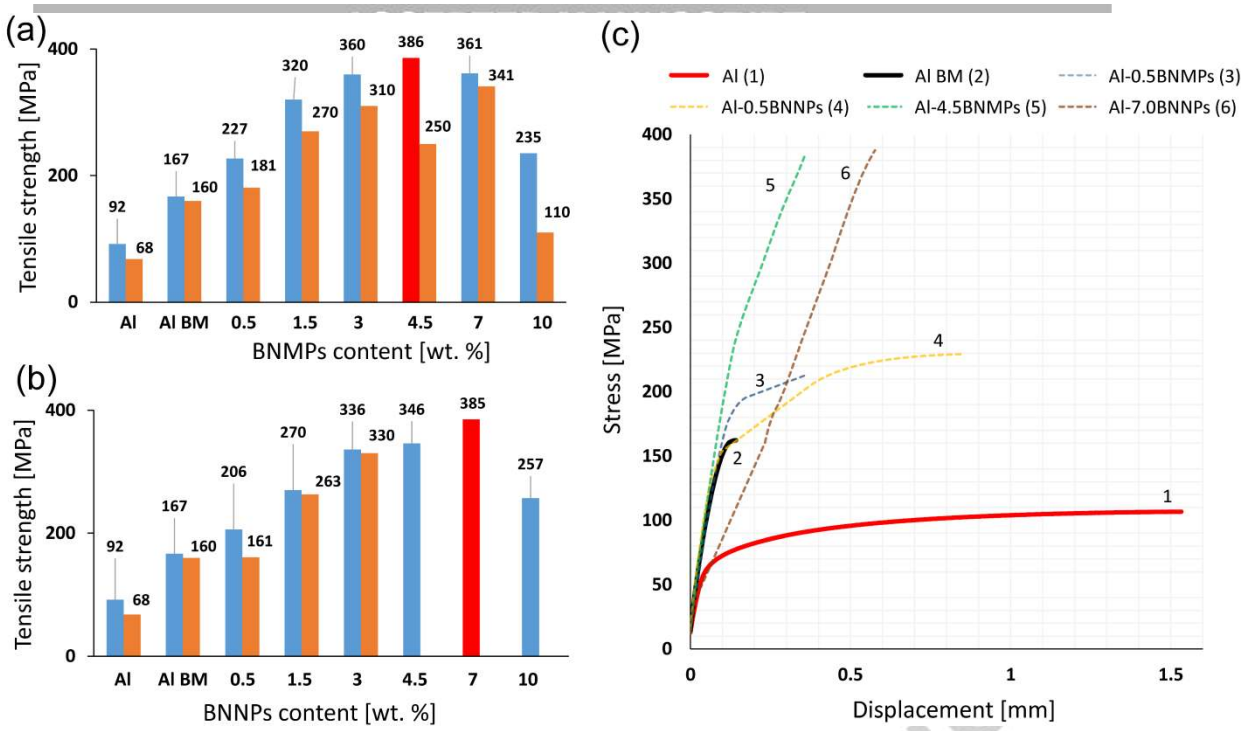

Fig. 1. Relationship between room temperature tensile properties (UTS-blue bars; $\sigma_{0.2}$ – orange bars, highest UTS values - red bars) and BN phase content for Al-BNMPs (a) and Al-BNNPs (b); Stress-displacement curves for pure Al and composites with the best mechanical properties (c).

2-column image

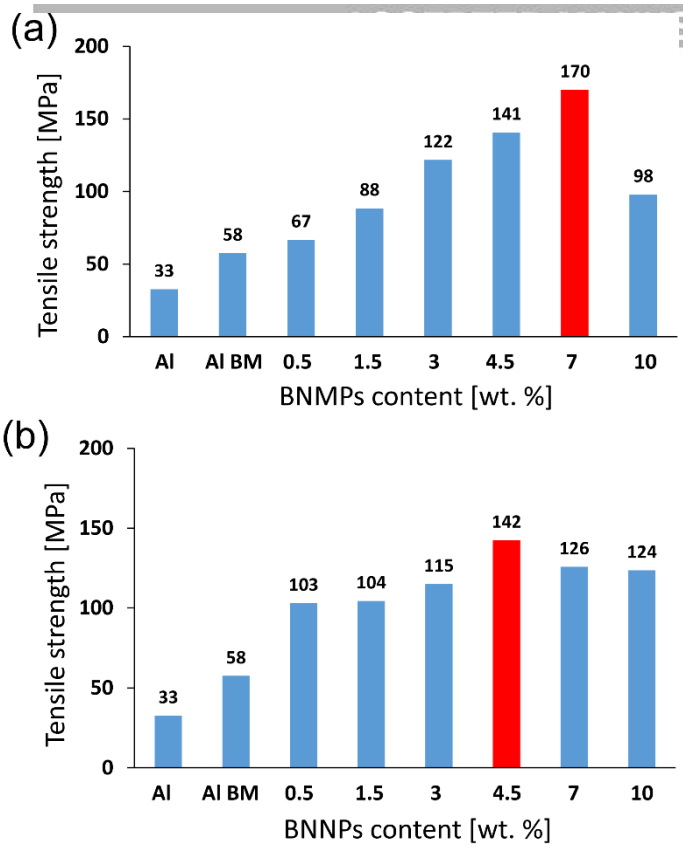

Fig. 2. Relationship between ultimate tensile strength at 500 °C and BN phase content for Al-BNMPs (a) and Al-BNNPs (b).

Single column image.

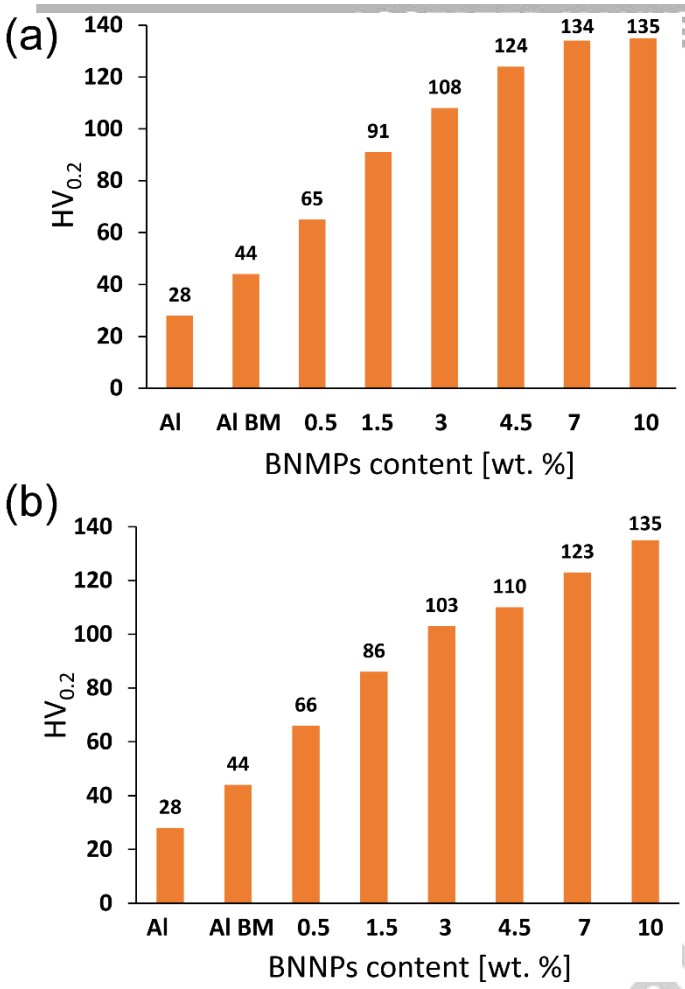

Fig. 3. Relationship between Vickers hardness and BN phase content for Al-BNMPs (a) and Al-BNNPs (b).

Single column image.

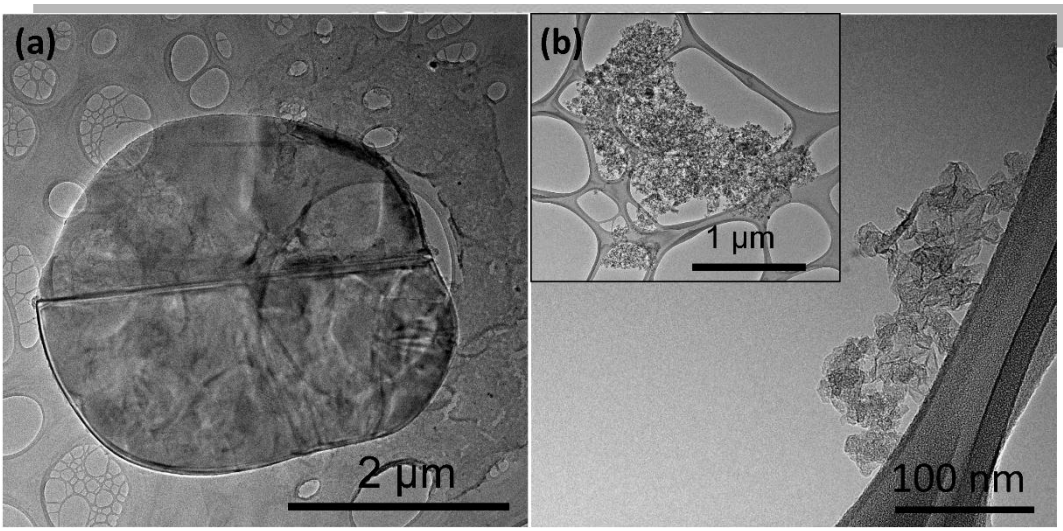

Fig. 4. TEM micrographs of a starting BNMP (a) and BNNPs (b).

1.5-column fitting image

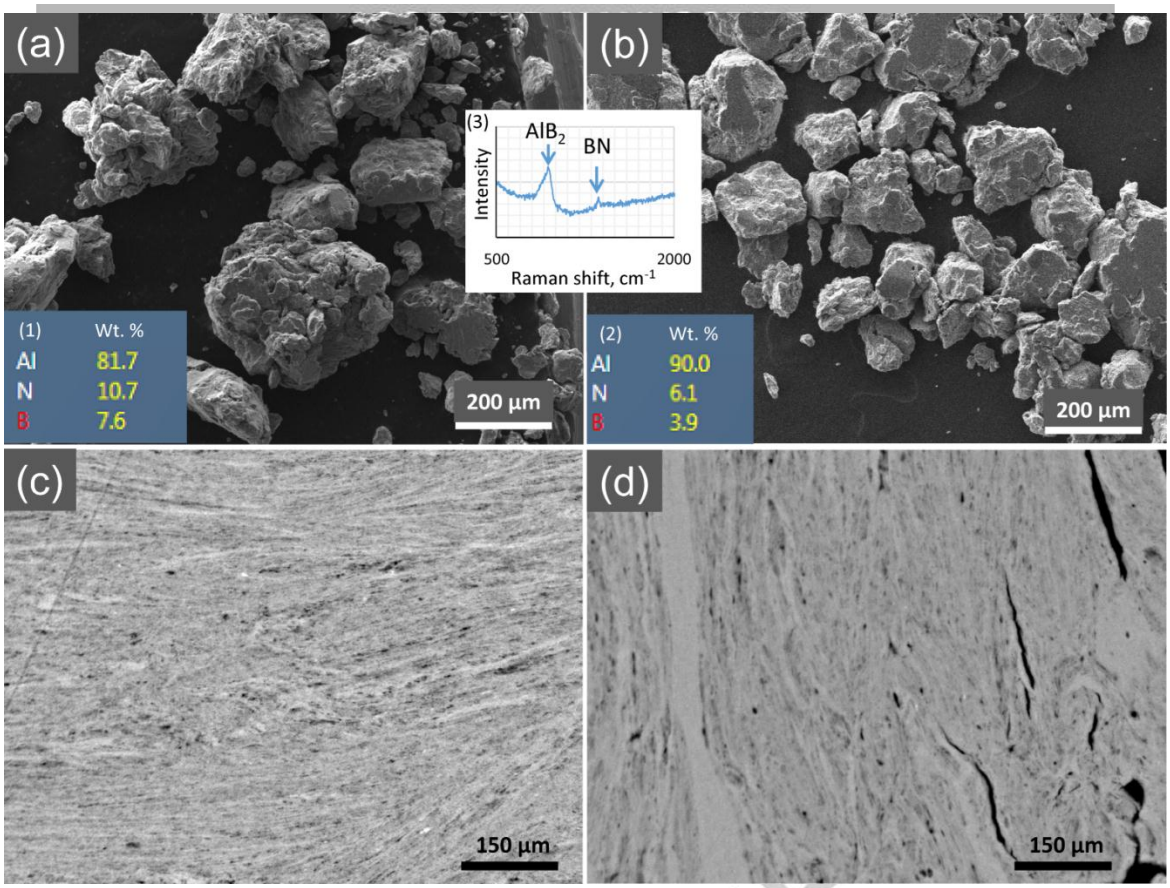

Fig. 5. SEM micrographs and results of EDS analysis (insets 1 and 2) for the powder mixtures of Al with 7 wt. % of BNMPs (a) and 7 wt. % of BNNPs (b). Inset 3 - Raman spectrum of an Al powder mixture with 7 wt. % of BNMPs. Cross-sectional SEM micrographs of Al powder mixture agglomerates with 7 wt. % of BNMPs (c) and 7 wt. % of BNNPs (d).

2-column image

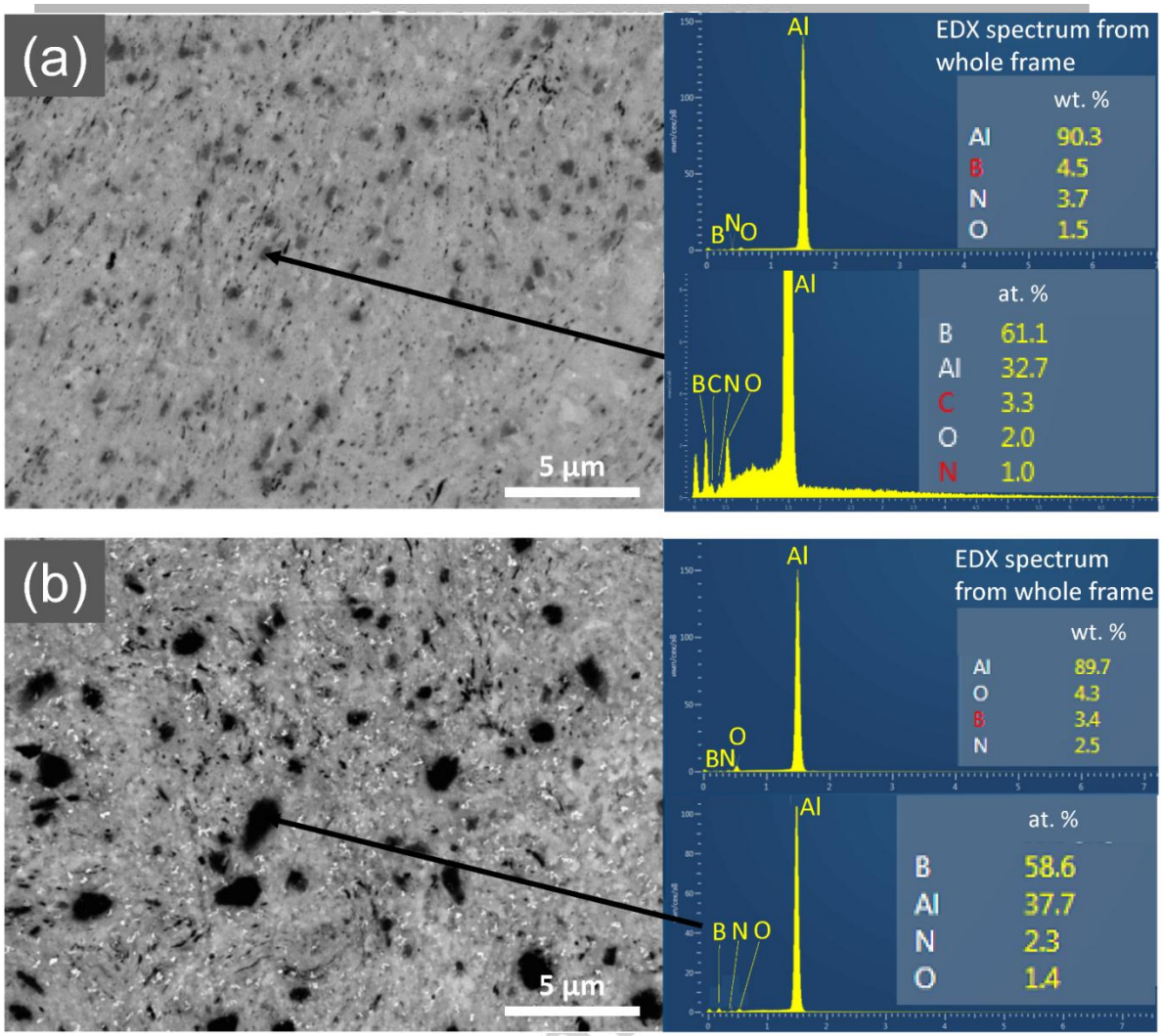

Fig. 6. SEM micrographs and results of spatially-resolved EDS analysis (right panels) for Al-4.5BNMPs (a) and Al-4.5BNNPs (b) SPS composites.

2-column image

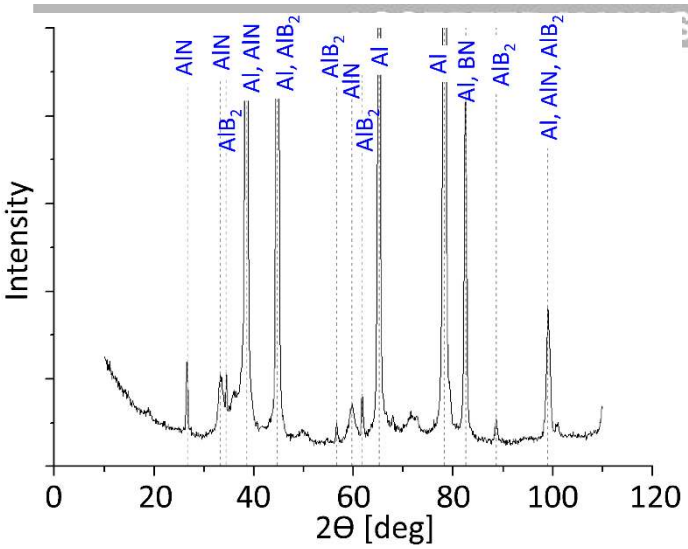

Fig. 7. XRD patterns of an Al-4.5BNMPs SPS composite.

Single column image.

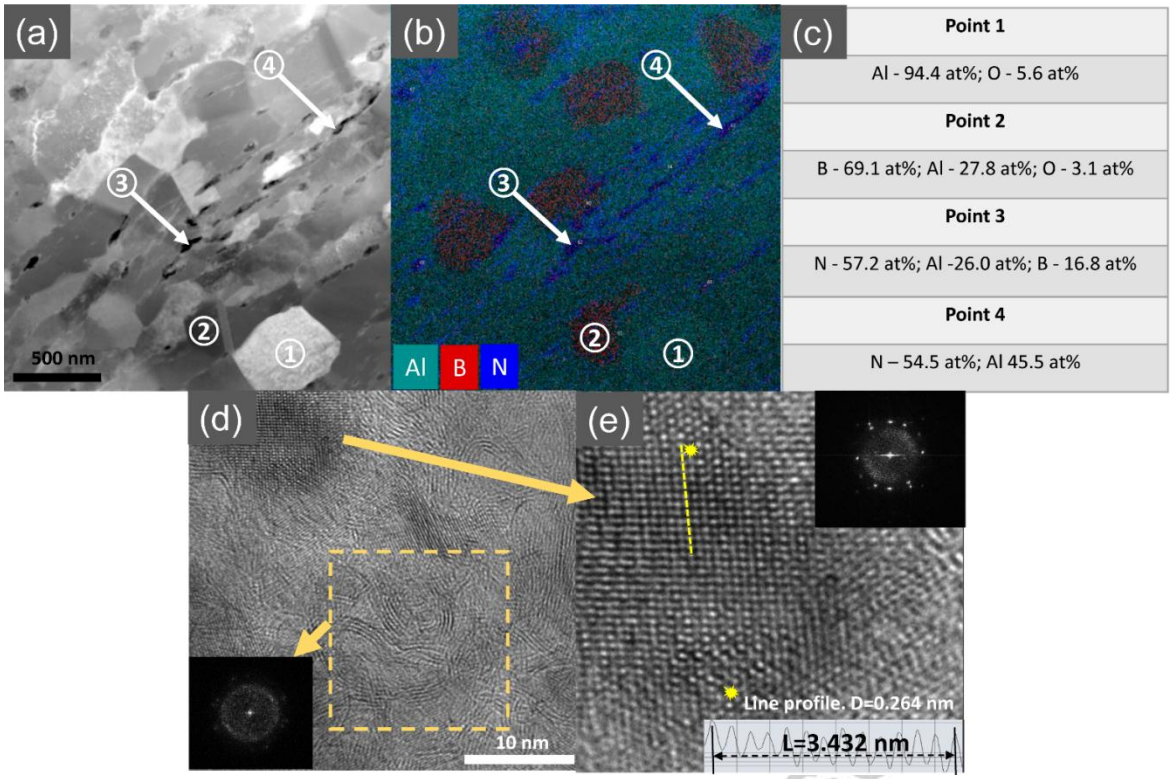

Fig. 8. HAADF image of an Al-4.5BNMPs sample (a); spatially-resolved elemental map (b); results of EDS chemical analysis in the selected spots (c); HRTEM image of a small black inclusion (d); HRTEM image of the AlN particle within the black inclusion (e); The corresponding FFT patterns are shown in the insets in (d) and (e).

2-column image

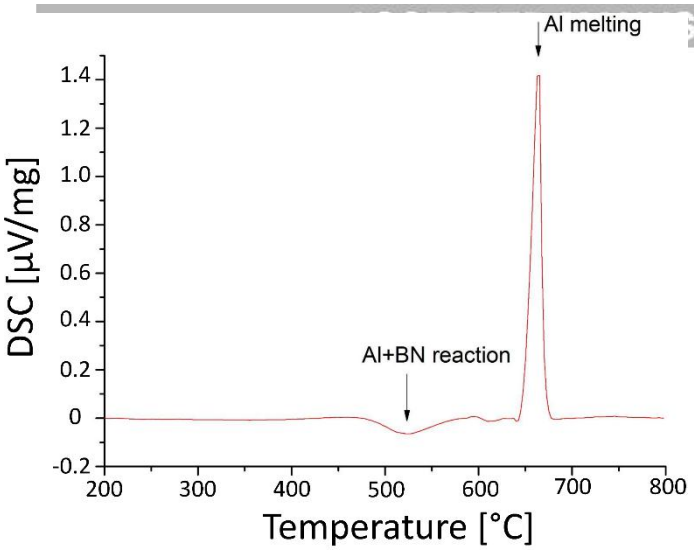

Fig. 9. DSC curve recorded during heating of a ball-milled Al-7.0BNMPs powder mixture.

Single column image.

Table 1 – Mechanical properties of Al based MMC prepared by various powder metallurgy methods

Ref.	Al-MMC Composition	Powder mixture preparation technique	Densification technique	Ultimate tensile strength (MPa)	Improvement (compared to matrix, %)
[32]	Al- 3 vol% MWCNT	Ultrasonic assisted wet mixing process	Cold-compacting and hot-pressing	421[32]	70
[33]	Al- 4.5 vol% MWCNT	High-energy ball milling (6 hours)	Hot rolling	619[33]	120
[34]	Al- 4.5 Wt.% MWCNT	*In situ* CVD synthesis, ball milling (1.5 hours)	Hot pressing and hot extrusion	420[34]	100
[35]	Al- 5.0 vol% MWCNT	Nanoscale dispersion	SPS and hot extrusion	194[35]	128
[36]	Al - 2 wt.% Al2O3 nanoparticles	High-energy ball milling (16 hours)	Hot extrusion	373[36]	20
[37]	Al - 4 wt.% Al2O3 nanoparticles	High-energy ball milling (5 hours)	Vacuum hot pressing	196[37]	37
[11]	Al - 6 wt.% Al2O3 nanoparticles	Wet mixing	Cold isotropic pressing and sintering	250[11]	67
[38]	Al - 10.0 wt.% Al2O3 microparticles	High-energy ball milling (1 hours)	Cold pressing and sintering	300[38]	90
[39]	Al - 1 vol.% SiC microparticles	SiC particles dispersed between Al strips	Accumulative roll bonding	243[39]	-
[21]	Al - 4.5 wt.% BN nanoparticles	Ultrasonic assisted wet mixing process	SPS	150[21]	50
[16]	Al - 5.0 wt.% BNNT	Ultrasonic assisted wet mixing process	High-pressure torsion technique	420[16]	90
This article	Al - 5.0 wt.% BN microparticles	High-energy ball milling (2 hours)	SPS	385	130